Mcl-1 and Bcl-x_L coordinately regulate megakaryocyte survival

*Marlyse A. Debrincat,[1,2] *Emma C. Josefsson,[1,2] *Chloé James,[1,2] Katya J. Henley,[1] Sarah Ellis,[3] Marion Lebois,[1] Kelly L. Betterman,[4] Rachael M. Lane,[1] Kelly L. Rogers,[5] Michael J. White,[1,2] Andrew W. Roberts,[1,2] Natasha L. Harvey,[4,6] Donald Metcalf,[1,2] and Benjamin T. Kile[1,2]

[1]Cancer and Hematology Division, The Walter and Eliza Hall Institute of Medical Research, Parkville, Australia; [2]Department of Medical Biology, University of Melbourne, Parkville, Australia; [3]Peter MacCallum Cancer Centre, East Melbourne, Australia; [4]Division of Haematology, Centre for Cancer Biology, SA Pathology, Adelaide, Australia; [5]Advanced Research Technologies, The Walter and Eliza Hall Institute of Medical Research, Parkville, Australia; and [6]School of Medicine, University of Adelaide, Adelaide, Australia

Mature megakaryocytes depend on the function of Bcl-x_L, a member of the Bcl-2 family of prosurvival proteins, to proceed safely through the process of platelet shedding. Despite this, loss of Bcl-x_L does not prevent the growth and maturation of megakaryocytes, suggesting redundancy with other prosurvival proteins. We therefore generated mice with a megakaryocyte-specific deletion of Mcl-1, which is known to be expressed in megakaryocytes. Megakaryopoiesis, platelet production, and platelet lifespan were unperturbed in *Mcl-1*$^{Pf4\Delta/Pf4\Delta}$ animals. However, treatment with ABT-737, a BH3 mimetic compound that inhibits the prosurvival proteins Bcl-2, Bcl-x_L, and Bcl-w resulted in the complete ablation of megakaryocytes and platelets. Genetic deletion of both Mcl-1 and Bcl-x_L in megakaryocytes resulted in preweaning lethality. Megakaryopoiesis in *Bcl-x*$^{Pf4\Delta/Pf4\Delta}$ *Mcl-1*$^{Pf4\Delta/Pf4\Delta}$ embryos was severely compromised, and these animals exhibited ectopic bleeding. Our studies indicate that the combination of Bcl-x_L and Mcl-1 is essential for the viability of the megakaryocyte lineage. (*Blood*. 2012;119(24):5850-5858)

Introduction

Megakaryocytes are large polyploid cells responsible for the production of blood platelets. They develop primarily in the BM and spleen. On reaching maturity, megakaryocytes extend long pseudopodial projections called proplatelets into the circulation, and it is from these structures that platelets are released.[1-3] Once born, platelets have a brief lifespan in the circulation: 10 days in humans, 5 days in mice.[4,5] In recent years, it has become apparent that this finite existence is governed by the interplay between members of the Bcl-2 protein family, the critical regulators of the "intrinsic" or "mitochondrial" apoptosis pathway.[6] Platelets depend on the prosurvival protein Bcl-x_L to maintain their viability.[7] Mutations in murine Bcl-x_L cause dose-dependent cell-intrinsic reductions in platelet lifespan.[7-9] Pharmacologic blockade of Bcl-x_L with the BH3 mimetic drugs ABT-737[10] or ABT-263[11] triggers platelet death[7,12-15] and thrombocytopenia in mice,[7,16] dogs,[15] and humans.[17,18]

The function of Bcl-x_L is to restrain the prodeath proteins Bak and Bax. When activated, Bak and Bax induce mitochondrial outer membrane permeabilization (MOMP), resulting in platelet apoptosis, which, at least in vitro, is characterized by cytochrome *c* release, caspase activation, and phosphatidylserine exposure.[12-15] At steady state in vivo, aged platelets that have escaped hemostatic consumption undergo Bak-mediated apoptosis and clearance from the circulation. Genetic deletion of Bak and Bax almost doubles platelet lifespan,[9] rescues the thrombocytopenia caused by loss of Bcl-x_L,[9] and renders platelets refractory to the effects of ABT-737.[13]

We recently demonstrated that Bcl-x_L is also essential for mature megakaryocytes to proceed safely through the process of platelet shedding.[9] In vitro, loss of Bcl-x_L triggers Bak- and Bax-mediated mitochondrial damage, caspase activation, and failure of proplatelet formation. In vivo, mature, shedding megakaryocytes lacking Bcl-x_L exhibit severe dysmorphology and produce grossly abnormal platelets that survive only hours in the circulation. Bcl-x_L is, however, dispensable for the growth and development of megakaryocytes, suggesting that other Bcl-2 family prosurvival proteins are necessary to promote survival during this process. Of the 5 prosurvival members of the Bcl-2 family,[6] 3 are known to be expressed in megakaryocytes: Bcl-2, Bcl-x_L, and Mcl-1.[9] Given its critical role in hematopoietic progenitors and lymphocytes,[19-21] we reasoned that Mcl-1 might contribute to the regulation of megakaryocyte survival. We therefore examined its role in the megakaryocyte lineage by conditionally deleting it in mice, alone, and in concert with Bcl-x_L.

Methods

Animals

Bcl-x floxed,[22] *Mcl-1* floxed,[7] and *Pf4-Cre*[23] mice have been previously described. All mutations had been backcrossed to wild-type C57BL/6 at least 10 generations before this study. All animal experiments complied with the regulatory standards of, and were approved by, the Walter and Eliza Hall Institute (WEHI) Animal Ethics Committee.

Materials

DMSO, propidium iodide, and anti–actin-HRP were purchased from Sigma-Aldrich. ABT-737 was provided by Abbott Laboratories. Q-VD-OPh was purchased from Alexis. The ECL system was from Millipore,

Submitted December 15, 2011; accepted February 23, 2012. Prepublished online as *Blood* First Edition paper, February 28, 2012; DOI 10.1182/blood-2011-12-398834.

*M.A.D., E.C.J., and C.J. contributed equally to this study.

There is an Inside *Blood* commentary on this article in this issue.

The publication costs of this article were defrayed in part by page charge payment. Therefore, and solely to indicate this fact, this article is hereby marked "advertisement" in accordance with 18 USC section 1734.

protease inhibitor cocktail, Complete was from Roche, 4%-12% Bis-Tris gels (NuPAGE), and AlexaFluor fluorochrome-conjugated secondary Abs were from Invitrogen. Abs used were X488 (Emfret Analytics GmbH and Co KG); fluorescently conjugated anti–mouse, CD41 (clone MWReg30), nonconjugated mouse anti–Bcl-x_L (clone 44; BD Biosciences); rat anti–Mcl-1 (clone 19C4-15; WEHI mAb Facility, Parkville, Australia); goat anti–human Prox1 (R&D Systems); rat anti–mouse endomucin (V.7C7; Santa Cruz Biotechnology Inc), polyclonal rabbit anti–human VWF (DakoCytomation), cleaved caspase-3 (Asp175, clone 5A1E), neuropilin2 (D39A5) XP rabbit mAb (Cell Signaling Technology); and the biotinylated goat anti–rabbit IgG Vectastain ABC kit and the Peroxidase substrate kit DAB (Vector Laboratories Inc).

Hematology

Automated cell counts were performed on blood collected from the retro-orbital plexus into Microtainer tubes containing EDTA (Sarstedt), using an Advia 2120 hematologic analyser (Siemens). Megakaryocytes were counted manually in sections of sternum and spleen stained with H&E with a minimum of 5-10 high-power fields (×200) analyzed. Morphometric analysis and enumeration of megakaryocytes was performed in images of H&E- and VWF-stained fetal livers by Metamorph image processing software (Version 7; Molecular Devices). Between 5 and 7 images per fetal liver were assessed. Hematopoietic progenitors were cultured as previously described.[24] Acute thrombocytopenia was induced by antiplatelet serum and assessed as described.[7]

Treatment of mice with ABT-737

Mice were injected intraperitoneally with 75 mg/kg ABT-737 given as a single dose as previously described.[7] A stock solution of ABT-737 (1 g/mL in DMSO) was diluted in a mixture of 30% propylene glycol, 5% Tween 80, 65% D5W (5% dextrose in water), pH 4-5. Blood and sternums were collected at time 0, 2, 2.5, 6, 24, 48, 72, and 96 hours after treatment. For transmission electron microscopic analyses, mice were killed at time 0 and 2.5 hours after treatment.

Megakaryocyte culture from fetal livers

Embryonic day 13.5 (E13.5) embryos were harvested into cold Dulbecco modified Eagle Kelso medium, 10% FCS. Fetal livers were dissected out and cell suspensions were prepared in PBS. A total of 5×10^5 cells/mL were seeded in 6-well plates into serum-free media (SFM) supplemented with 100 ng/mL murine thrombopoietin (TPO; WEHI). Cells were cultured for 3-5 days at 37°C, 5% CO_2. To isolate dense viable mature megakaryocytes, cells were overlaid on a discontinuous BSA (Fraction V; Invitrogen) density gradient (3, 1.5, 0%), and cells were harvested in the 3% layer.

Proplatelet formation assay

Large fetal liver–derived megakaryocytes were seeded in 96-well plates 300-500 cells/well into SFM supplemented with TPO. Megakaryocytes displaying proplatelets were counted by microscopy and percentage calculated by dividing the number of proplatelet forming megakaryocytes with the total number of cells each day.

Megakaryocyte ploidy

BM was harvested from 8- to 10-week-old mice and megakaryocyte ploidy was studied with propidium iodide as previously described.[25]

Serum thrombopoietin

Serum TPO levels were measured using the Quantikine Mouse TPO Immunoassay kit (R&D Systems) according to the manufacturer's instructions.

Caspase activity and viability assays

Megakaryocytes were harvested from BSA gradients, counted and reseeded in SFM with TPO into 96-well plates, and returned to the 37°C incubator after the addition of ABT-737 (5μM), the caspase inhibitor, Q-VD-OPh (QVD; 50μM), or vehicle control DMSO if not otherwise stated. Caspase-Glo 3/7 reagents (Promega) were added to the cells after 5 hours. The luminescence of each sample was determined in a plate-reading LumiSTAR Galaxy luminometer (BMG Labtech) as directed by manufacturer. Alternatively, Celltiter Glo reagents (Promega) were added after 24 hours to measure ATP levels.

Platelet preparation

Blood was obtained by cardiac puncture into 0.1 volume of Aster Jandl citrate-based anticoagulant (85mM sodium citrate, 69mM citric acid, 20 mg/mL glucose, pH 4.6).[26] Mouse platelet-rich plasma (PRP) was obtained by centrifugation of the murine blood at 125*g* for 8 minutes, followed by centrifugation of the supernatant buffy coat at 125*g* for 8 minutes. Mouse platelets were washed by 2 sequential centrifugations at 860*g* for 5 minutes in 140mM NaCl, 5mM KCl, 12mM trisodium citrate, 10mM glucose, 12.5mM sucrose, pH 6.0 (buffer A). The platelet pellet was resuspended in 10mM HEPES, 140mM NaCl, 3mM KCl, 0.5mM $MgCl_2$, 10mM glucose, and 0.5mM $NaHCO_3$, pH 7.4 (buffer B).

Platelet turnover studies

Platelet lifespan was assessed with platelet-specific X488 injected intravenously and platelet lifespan was measured in PRP by flow cytometry as previously described.[27]

SDS-PAGE and Western blot analysis

Platelets and megakaryocytes were lysed in NP40 lysis buffer or RIPA buffer, respectively. Proteins were separated on 4%-12% Bis-Tris gels (NuPAGE; Invitrogen) under reducing conditions, transferred onto Immobilon-P membranes (Micron Separation), and immunoblotted with various Abs, followed by secondary HRP-conjugated Abs and ECL.

Electron microscopy

Transmission electron microscopy was performed after fixation and decalcification of murine femurs as described.[25]

Immunofluorescent staining

Embryos were fixed in 4% paraformaldehyde. Paraffin sections (4 μm) were dewaxed and rehydrated, before heat-mediated Ag retrieval in citrate buffer (pH 6.5). Paraffin-embedded sections were blocked using PBS containing 0.3% (v/v) Tween 20 and 1% (w/v) BSA, followed by overnight incubation at 4°C with primary Abs; rat anti–mouse endomucin (V.7C7; stains blood vascular, but not lymphatic vascular endothelial cells), goat anti–human Prox1 (stains lymphatic endothelial cells), and neuropilin2 (D39A5) XP rabbit mAb (stains venous and lymphatic endothelial cells). Sections were washed extensively using PBS and incubated with AlexaFluor fluorochrome–conjugated secondary Abs for 2 hours. Samples were mounted in Gel/Mount Aqueous Mounting Medium with Anti-Fading Agents (Biomeda). Z-stack images were obtained using a Bio-Rad Radiance 2100 confocal microscope equipped with 3 lasers (488-nm Argon-ion laser, HeNe 543-nm green laser, 637-nm red diode laser) attached to an Olympus IX70 inverted microscope with UPlanApo 10×/0.40 ∞/0.17 and UApo/340 20×/0.70W ∞/0.17 (Olympus) objectives. Image acquisition was performed at room temperature using LaserSharp 2000 software (Version 5.2; Bio-Rad). Adobe Photoshop CS5 (Version 12.0) was used for subsequent image processing.

IHC

Spleens were fixed in 10% formalin and embryos in 4% paraformaldehyde and embedded in paraffin. Sections were dewaxed and Ag retrieved by heating slides in 90°C citrate buffer (pH 6.0) for 20 minutes. Before staining, slides were quickly rinsed in 25mM Tris pH 7.5. Endogenous peroxidase activity was quenched with 3% H_2O_2 in dH_2O for 10 minutes. Tissues were circled with a wax pen and blocked for 10 minutes in 10% bovine calf serum, 1% BSA, and thereafter washed in PBS. Primary Abs directed against VWF (localized in α-granules in megakaryocytes and platelets) or active caspase-3 were incubated 1 hour at room temperature

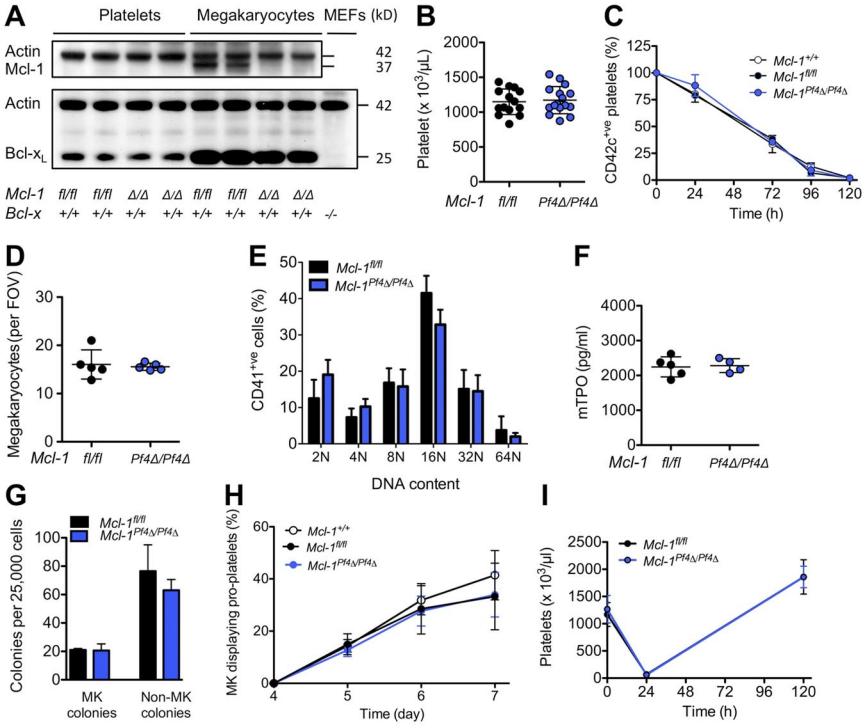

Figure 1. Loss of Mcl-1 does not affect platelet production. (A) Western blot of protein lysates from platelets and fetal liver–derived megakaryocytes. E13.5 fetal liver cells were cultured in SFM in thrombopoietin for 5 days, and then large megakaryocytes were purified from a BSA gradient. Mcl-1 was efficiently deleted in mouse megakaryocytes. Its loss did not influence Bcl-x_L protein levels. Mcl-1 expression was below detection level in control blood platelets under the conditions used. Δ/Δ indicates *platelet factor 4 (Pf4)* Cre-specific deletion. Actin was used as a control for protein loading. Negative control for Bcl-x_L was *Bcl-x*$^{-/-}$ mouse embryonic fibroblast (MEF) lysate. (B) Blood platelet counts were normal in *Mcl-1*$^{Pf4\Delta/Pf4\Delta}$ mice and *Mcl-1*$^{fl/fl}$ control mice at 7 weeks of age. Data represent mean ± SD. Each symbol represents an individual mouse. (C) Platelet survival curves in *Mcl-1*$^{Pf4\Delta/Pf4\Delta}$, *Mcl-1*$^{fl/fl}$, and *Mcl-1*$^{+/+}$ mice. Platelets were labeled via IV injection of a DyLight 488–conjugated anti-GPIbβ (CD42c) Ab. Data represent mean ± SD n = 4 *Mcl-1*$^{+/+}$; n = 5 *Mcl-1*$^{Pf4\Delta/Pf4\Delta}$; n = 1 *Mcl-1*$^{fl/fl}$ mice per group. (D) Morphologically recognizable megakaryocytes in H&E-stained sections of BM from *Mcl-1*$^{Pf4\Delta/Pf4\Delta}$ and *Mcl-1*$^{fl/fl}$ mice. Each symbol represents the mean number per field of view (FOV; ×200) from 5 fields per individual mouse. Data represent overall mean ± SD. (E) Ploidy distribution profile of CD41$^+$ BM cells in *Mcl-1*$^{Pf4\Delta/Pf4\Delta}$ and *Mcl-1*$^{fl/fl}$ mice determined by flow cytometry. Data represent mean ± SD; n = 4-6 mice per genotype. (F) Serum thrombopoietin levels in *Mcl-1*$^{Pf4\Delta/Pf4\Delta}$ and *Mcl-1*$^{fl/fl}$ mice. Each symbol represents an individual mouse. Data represent mean ± SD. (G) Hematopoietic progenitor cell numbers in adult mice. Twenty-five thousand BM cells were cultured with stem cell factor, IL-3, and erythropoietin in semisolid agar for 7 days. Non-megakaryocyte (MK) colonies represent the total of blast, granulocyte, mixed granulocyte/macrophage, macrophage, and eosinophil colonies. Data represent ± SEM n = 2 *Mcl-1*$^{fl/fl}$; n = 3, *Mcl-1*$^{Pf4\Delta/Pf4\Delta}$. (H) Proplatelet formation in cultured megakaryocytes (MK). E13.5 fetal liver cells were cultured in SFM in thrombopoietin for 3 days. On day 4, large megakaryocytes were purified from a BSA gradient and reseeded to investigate proplatelet formation. Data are presented as the percentage of proplatelet forming megakaryocytes per day and represent mean ± SEM, n = 5 *Mcl-1*$^{+/+}$; n = 5, *Mcl-1*$^{Pf4\Delta/Pf4\Delta}$; n = 3, *Mcl-1*$^{fl/fl}$ biological replicates. (I) Blood platelet counts in response to antiplatelet serum (APS)–induced thrombocytopenia. No significant difference was detected. Data represent mean ± SD; n = 5 mice per genotype at each time point.

(RT). Slides were washed followed with secondary biotinylated goat anti–rabbit Ab for 45 minutes at RT. Slides were rinsed and incubated with Vectastain ABC kit mix for 30 minutes at RT, followed by a washing step and Peroxidase substrate kit DAB solution from Vector Laboratories for 6-8 minutes as directed by manufacturer. The slides were washed in water, counterstained with hematoxylin, and mounted. Images were acquired on a Nikon Eclipse E600 microscope equipped with AxioCam MRc5 (Zeiss) and AxioVision 4.8. Scale bars were inserted with ImageJ 1.42q.

Statistical analyses

Statistical significance between 2 treatment groups was analyzed using an unpaired Student *t* test with 2-tailed *P* values. One-way ANOVA with the Bonferroni multiple comparison test was applied where appropriate (GraphPad Prism Software Version 5.0a). $*P < .05$; $**P < .005$; $***P < .0001$ or as otherwise stated. Data are presented as mean ± SEM or SD (where indicated).

Results

Mcl-1 is dispensable for normal megakaryopoiesis and platelet lifespan

Mice harboring a floxed allele of *Mcl-1*[7] were crossed with *Pf4-Cre* transgenic animals in which Cre recombinase is expressed under the control of the *Platelet factor 4* promoter.[23] At weaning, *Mcl-1*$^{Pf4\Delta/Pf4\Delta}$ mice were present in the expected Mendelian ratios and were outwardly healthy. Western blot analysis confirmed that Mcl-1 was efficiently deleted from megakaryocytes (Figure 1A). Platelet counts and platelet survival curves in *Mcl-1*$^{+/+}$, *Mcl-1*$^{fl/fl}$, and *Mcl-1*$^{Pf4\Delta/Pf4\Delta}$ mice were indistinguishable (Figure 1B-C; Table 1). Megakaryocyte numbers, morphology, and ploidy were normal (Figure 1D-E). Serum thrombopoietin levels were unchanged (Figure 1F), and enumeration of megakaryocyte progenitors in semisolid agar cultures revealed no differences (Figure 1G). In vitro, the ability of cultured Mcl-1–deficient megakaryocytes to elaborate proplatelets was unimpaired (Figure 1H). In vivo, *Mcl-1*$^{Pf4\Delta/Pf4\Delta}$ mice mounted a wild-type response to experimentally induced thrombocytopenia (Figure 1I). Together, these data demonstrate that Mcl-1 is dispensable for normal megakaryopoiesis, platelet production, and platelet lifespan.

ABT-737 induces cell death in Mcl-1–deficient megakaryocytes

The BH3 mimetic compound ABT-737 binds to and inhibits the prosurvival proteins Bcl-2, Bcl-x_L, and Bcl-w.[10] In cultured wild-type megakaryocytes, it induces a significant degree of Bak/Bax-dependent apoptosis.[9] To probe any potential functional redundancy between Mcl-1 and Bcl-x_L, we therefore exposed *Mcl-1*$^{+/+}$ and *Mcl-1*$^{Pf4\Delta/Pf4\Delta}$ fetal liver–derived megakaryocytes to ABT-737.

Table 1. Blood counts from adult *Mcl-1*$^{+/+}$, *Mcl-1*$^{fl/fl}$, and *Mcl-1*$^{Pf4\Delta/Pf4\Delta}$ mice at steady state and 48 hours after single-dose ABT-737 treatment

	Untreated			ABT-737		
	Mcl-1$^{+/+}$, n = 13	*Mcl-1*$^{fl/fl}$, n = 20	*Mcl-1*$^{Pf4\Delta/Pf4\Delta}$, n = 20	*Mcl-1*$^{+/+}$, n = 7	*Mcl-1*$^{fl/fl}$, n = 6	*Mcl-1*$^{Pf4\Delta/Pf4\Delta}$, n = 6
Platelets, $\times 10^6$/mL	1228 ± 263	1092 ± 150	1156 ± 235	644 ± 198	686 ± 252	99 ± 106*
MPV, fL	7.4 ± 1.0	7.7 ± 0.7	7.6 ± 0.9	7.1 ± 0.4	7.1 ± 0.9	9.9 ± 3.3
PDW, %	50.3 ± 4.4	52.8 ± 3.9	51.7 ± 4.8	47.0 ± 4.2	53.0 ± 6.6	88.6 ± 22.4*
Erythrocytes, $\times 10^9$/mL	10.8 ± 0.4	11.0 ± 0.6	11.2 ± 0.4	10.9 ± 0.3	11.3 ± 0.3	11.0 ± 2.4
Hematocrit, %	50.4 ± 2.3	52.9 ± 4.7	52.9 ± 3.7	55.4 ± 2.3	50.4 ± 1.4	48.7 ± 10.0
Neutrophils, $\times 10^6$/mL	0.9 ± 0.6	1.0 ± 0.3	1.2 ± 0.5	0.6 ± 0.2	0.9 ± 0.2	1.0 ± 0.3†
Lymphocytes, $\times 10^6$/mL	7.3 ± 1.7	9.7 ± 1.6*	9.7 ± 1.3*	2.9 ± 1.5	5.2 ± 1.6	4.4 ± 1.9
Monocytes, $\times 10^6$/mL	0.2 ± 0.1	0.2 ± 0.1	0.2 ± 0.1	0.1 ± 0.0	0.1 ± 0.0	0.2 ± 0.0
Eosinophils, $\times 10^6$/mL	0.2 ± 0.1	0.2 ± 0.1	0.2 ± 0.1	0.2 ± 0.0	0.2 ± 0.0	0.2 ± 0.1

Data represent mean ± SD, 1-way ANOVA with Bonferroni multiple comparison test. *Mcl-1*$^{fl/fl}$ *and Mcl-1*$^{Pf4\Delta/Pf4\Delta}$ *mice were compared to Mcl-1*$^{+/+}$ mice according to treatment groups.

MPV indicates mean platelet volume; and PDW, platelet distribution width.

*$P < .0001$.

†$P < .005$.

Mcl-1–deficient cells were markedly more sensitive to the drug, exhibiting a 3- to 4-fold increase in the activity of the apoptotic effector caspases-3/7 relative to wild type (Figure 2A). ATP levels, a marker of mitochondrial function and cell viability, were dramatically decreased after 24 hours of culture (Figure 2B). This prompted us to examine the effects of ABT-737 in vivo.

Mcl-1$^{+/+}$, *Mcl-1*$^{fl/fl}$, and *Mcl-1*$^{Pf4\Delta/Pf4\Delta}$ mice were given a single IP 75 mg/kg dose of ABT-737 and cohorts taken for analysis over the course of 4 days. As expected, platelet counts in all groups fell, but the nadir in *Mcl-1*$^{Pf4\Delta/Pf4\Delta}$ animals was deeper and more prolonged, with platelets essentially undetectable at 6-48 hours after treatment (Figure 2C). BM megakaryocytes in these mice were completely absent at the 6- and 24-hour time points, in stark contrast to *Mcl-1*$^{+/+}$ and *Mcl-1*$^{fl/fl}$ controls in which megakaryocyte numbers were stable (Figure 2D). Given the kinetics of cell loss, and the fact that megakaryocyte progenitors were unaffected by

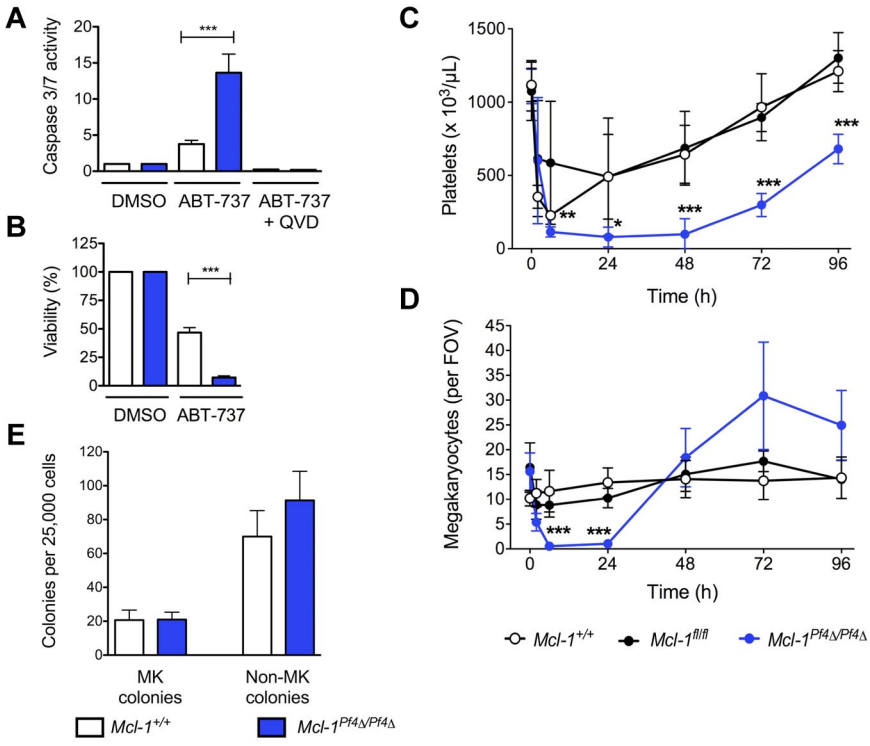

Figure 2. ABT-737 induces cell death in Mcl-1–deficient megakaryocytes. (A) Caspase 3/7 activity in fetal liver–derived megakaryocytes treated with ABT-737. Fetal livers were cultured in SFM plus TPO for 3 days. Large megakaryocytes were purified from a BSA gradient and reseeded. Caspase activity was measured 5 hours after treatment with ABT-737 (5μM) or vehicle (DMSO) with or without the caspase inhibitor, QVD, using the Promega Caspase-Glo assay. Data represent fold increase compared with control ± SEM, n = 2 technical replicates for each genotype. Representative of 4-5 independent experiments. (B) Mitochondrial function in fetal liver–derived megakaryocytes treated with ABT-737. ATP levels in fetal liver–derived megakaryocytes were measured 24 hours after reseeding and treating with ABT-737 (5μM) or vehicle (DMSO) using the CellTiter-Glo assay system. DMSO control was set as 100% for each genotype. Data represents mean ± SEM, n = 4-9 independent experiments. ***$P < .0001$. (C) Peripheral blood platelet counts in *Mcl-1*$^{+/+}$, *Mcl-1*$^{fl/fl}$, and *Mcl-1*$^{Pf4\Delta/Pf4\Delta}$ mice treated with a single IP injection of ABT-737 (75 mg/kg). Cohorts of mice were bled at indicated time points to determine platelet counts; n = 3-6 mice per genotype at 2 hours after treatment, n = 3-8 at 6 hours, n = 5-9 at 24 hours and n = 6-7 at 48 hours. Data represent mean ± SD. (D) Megakaryocyte counts in *Mcl-1*$^{+/+}$, *Mcl-1*$^{fl/fl}$, and *Mcl-1*$^{Pf4\Delta/Pf4\Delta}$ mice treated with a single IP injection of ABT-737 (75 mg/kg). Data represent mean number of BM megakaryocytes per field of view (FOV; ×200) from at least 5 fields per individual mouse; n = 3-6 mice per genotype at each time point. Data represent mean ± SD. (E) Hematopoietic progenitor cell numbers in adult mice 2.5 hours after treatment with ABT-737. Twenty-five thousand BM cells were cultured with stem cell factor, IL-3, and erythropoietin in semisolid agar for 7 days. Non-megakaryocyte (MK) colonies represent the total of blast, granulocyte, mixed granulocyte/macrophage, macrophage, and eosinophil colonies. Data represent ± SEM; n = 3, *Mcl-1*$^{+/+}$; n = 3, *Mcl-1*$^{Pf4\Delta/Pf4\Delta}$.

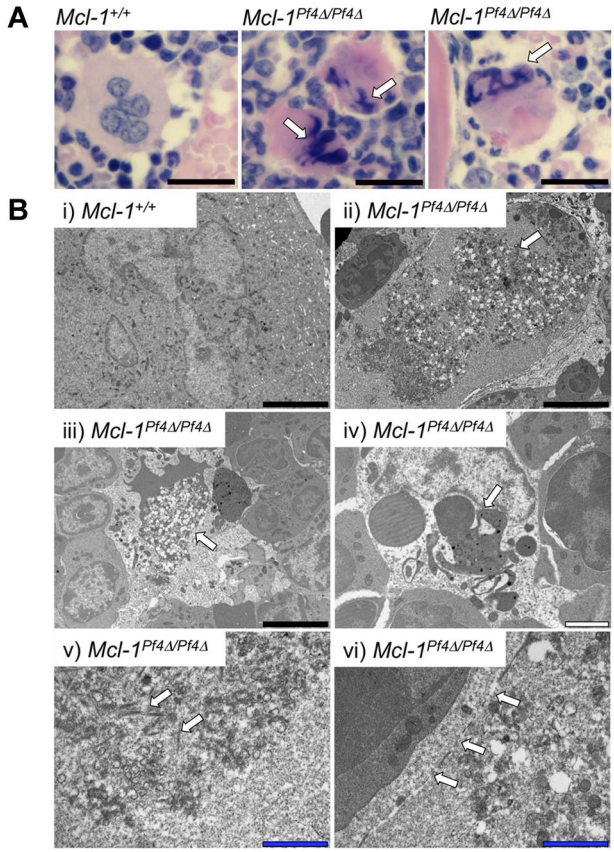

Figure 3. Apoptosis of Mcl-1–deficient megakaryocytes in vivo. (A) H&E-stained sternum sections from ABT-737–treated *Mcl-1*$^{+/+}$ and *Mcl-1*$^{Pf4\Delta/Pf4\Delta}$ mice, 2.5 hours after treatment. Pyknotic nuclei are indicated by white arrows. Scale bar: 20 μm. (Bii-vi) Representative transmission electron microscope images of BM sections showing aberrant megakaryocyte morphology and death in *Mcl-1*$^{Pf4\Delta/Pf4\Delta}$ mice 2.5 hours after ABT-737 treatment. White arrows highlight abnormal characteristics in *Mcl-1*$^{Pf4\Delta/Pf4\Delta}$ megakaryocytes not observed in wild-type controls (i). (i-iii) Examples of megakaryocytes displaying cytoplasmic vacuolization. (iv) Dysmorphic megakaryocyte nucleus. (v) Accumulation of short filamentous bundles within megakaryocyte. (vi) Megakaryocyte displaying fragmentation of plasma membrane. Black scale bars: 5 μm; white scale bar: 2 μm; blue scale bar: 1 μm.

ABT-737 treatment (Figure 2E), these results suggested that the drug was directly toxic to Mcl-1–deficient megakaryocytes.

In H&E sections of *Mcl-1*$^{Pf4\Delta/Pf4\Delta}$ BM taken 2.5 hours after ABT-737 administration, megakaryocytes exhibited nuclear pyknosis and cytoplasmic dysmorphology (Figure 3A). More detailed transmission electron microscopy studies revealed megakaryocytes at various stages of degeneration (Figure 3B). Many cells showed condensation of organelles toward the cell center, and an accumulation of short filamentous bundles, suggestive of cytoskeletal collapse. Nuclear chromatin was condensed, with nuclei forming striking multilobed thread-like structures. In some cases, fragmentation of the plasma membrane was observed. The cytoplasm of cells that appeared to be in the later stages of cell death was highly vacuolated and dissipated. Macrophages were often present at these sites, many containing spherical structures presumed to be apoptotic bodies.

Megakaryocyte-specific deletion of Mcl-1 and Bcl-x$_L$ compromises megakaryocyte survival

Our results suggested that the combination of Bcl-x$_L$ and Mcl-1 is essential for the viability of the megakaryocyte lineage. We therefore created mice deficient for both proteins in megakaryocytes by crossing *Mcl-1*$^{Pf4\Delta/Pf4\Delta}$ animals with those carrying a floxed allele of *Bcl-x*.[22] The result was preweaning lethality; no *Bcl-x*$^{Pf4\Delta/Pf4\Delta}$ *Mcl-1*$^{Pf4\Delta/Pf4\Delta}$ double knockout mice were recovered at 21 days of age (0 weaned/13 expected). We did observe *Bcl-x*$^{Pf4\Delta/Pf4\Delta}$ *Mcl-1*$^{+/Pf4\Delta}$ animals at weaning, but at only ~ 30% the expected rate (15 weaned/47 expected). Like their *Bcl-x*$^{Pf4\Delta/Pf4\Delta}$ *Mcl-1*$^{+/+}$ littermates, adult *Bcl-x*$^{Pf4\Delta/Pf4\Delta}$ *Mcl-1*$^{+/Pf4\Delta}$ survivors exhibited platelet counts ~ 5% of wild-type levels, and elevations in mean platelet volume (Figure 4A). This was consistent with the prior demonstration that, in the absence of Bcl-x$_L$, mature megakaryocytes are unable to restrain proapoptotic Bak and Bax.[9] As a result, they undergo an abortive shedding process that releases morphologically aberrant platelets and fragments of dying megakaryocyte cytoplasm into the circulation. Because platelets depend on Bcl-x$_L$ for survival,[7] those platelets that are produced have a lifespan of only 5 hours (cf 5 days in wild-type). The combination of late-stage megakaryocyte death and reduced platelet survival results in severe macrothrombocytopenia.[9]

Megakaryocytes only become specifically dependent on Bcl-x$_L$ on reaching maturity and the point at which proplatelet formation begins. Accordingly, and as previously documented,[9] megakaryopoiesis was expanded in *Bcl-x*$^{Pf4\Delta/Pf4\Delta}$ *Mcl-1*$^{+/+}$ mice, with a 4-fold increase in megakaryocyte numbers, relative to wild type, observed in the BM (Figure 4A). In *Bcl-x*$^{Pf4\Delta/Pf4\Delta}$ *Mcl-1*$^{+/Pf4\Delta}$ animals, however, only a 2-fold increase in megakaryocytes was apparent. On closer examination of H&E sections, a subset of the megakaryocyte population in this genotypic class exhibited a phenotype strikingly similar to that of megakaryocytes in *Mcl-1*$^{Pf4\Delta/Pf4\Delta}$ mice after ABT-737 treatment, with nuclear pyknosis and cytoplasmic dysmorphology clearly evident (Figure 4B). Immunohistochemical staining showed that these cells were positive for the active form of the apoptotic executioner caspase, caspase-3 (Figure 4C). Transmission electron microscopy studies revealed condensation of organelles, highly vacuolated cytoplasm, and a lack of organized demarcation membrane system (Figure 4D), confirming the morphologic parallels between *Bcl-x*$^{Pf4\Delta/Pf4\Delta}$ *Mcl-1*$^{+/Pf4\Delta}$ megakaryocytes and Mcl-1–deficient megakaryocytes treated with ABT-737. Together, these data indicate that Bcl-x$_L$ and Mcl-1 coordinately regulate the survival of maturing megakaryocytes. Deletion of Bcl-x$_L$ impairs survival at the point of platelet shedding. The additional loss of 1 allele of Mcl-1 reduces the prosurvival load such that developing megakaryocytes are also prone to undergoing apoptotic death. This reduces megakaryocyte numbers in *Bcl-x*$^{Pf4\Delta/Pf4\Delta}$ *Mcl-1*$^{+/Pf4\Delta}$ mice, and, presumably, compromises hemostasis even more severely than in *Bcl-x*$^{Pf4\Delta/Pf4\Delta}$ *Mcl-1*$^{+/+}$ counterparts. In support of this notion, *Bcl-x*$^{Pf4\Delta/Pf4\Delta}$ *Mcl-1*$^{+/Pf4\Delta}$ survivors were anemic (Figure 4A), consistent with chronic low-level bleeding.

Megakaryocyte-specific deletion of Mcl-1 and Bcl-x$_L$ results in hemorrhage and lethality

Analysis of timed matings indicated that, at E12.5, *Bcl-x*$^{Pf4\Delta/Pf4\Delta}$ *Mcl-1*$^{+/+}$, *Bcl-x*$^{Pf4\Delta/Pf4\Delta}$ *Mcl-1*$^{+/Pf4\Delta}$, and *Bcl-x*$^{Pf4\Delta/Pf4\Delta}$ *Mcl-1*$^{Pf4\Delta/Pf4\Delta}$ embryos were present in Mendelian ratios. However, there were obvious signs of ectopic bleeding in all 3 genotypic classes, in contrast to wild-type embryos where we observed none (Figure 5A). Given previous reports demonstrating the requirement for platelets in the separation of blood and lymphatic vessels,[28,29] we conducted immunostaining studies using Abs to endomucin, Prox1, and neuropilin2 to distinguish blood and lymphatic vessels. Our analyses revealed blood-filled lymph sacs and lymphatic vessels in 2 of 3 *Bcl-x*$^{Pf4\Delta/Pf4\Delta}$ *Mcl-1*$^{+/+}$ and 3 of 4 *Bcl-x*$^{Pf4\Delta/Pf4\Delta}$ *Mcl-1*$^{Pf4\Delta/Pf4\Delta}$ embryos (Figure 5Biii-v), which were not apparent in 3 wild-type controls (Figure 5Bi-ii). In addition, hemorrhaging was observed in

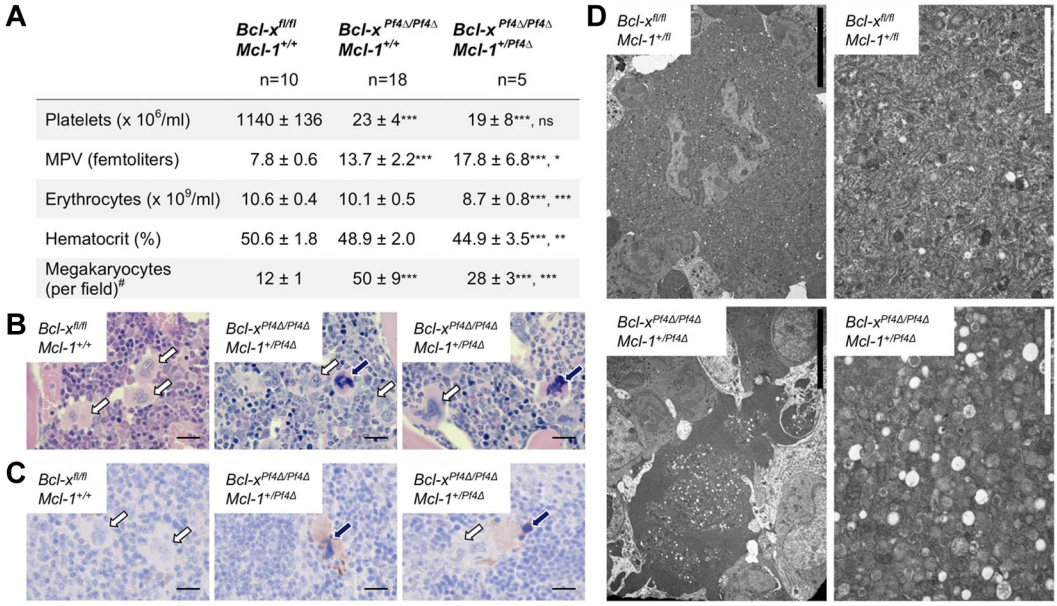

Figure 4. Megakaryocyte-specific loss of *Bcl-x* and 1 allele of *Mcl-1* predisposes megakaryocytes to cell death. (A) Peripheral blood counts from 7-week-old mice. Data represent mean ± SD, 1-way ANOVA with Bonferroni multiple comparison test. MPV indicates mean platelet volume. *Bcl-x*$^{Pf4\Delta/Pf4\Delta}$ *Mcl-1*$^{+/Pf4\Delta}$ mice were firstly compared with *Bcl-x*$^{fl/fl}$ *Mcl-1*$^{+/+}$ controls, and secondly to *Bcl-x*–deficient *Bcl-x*$^{Pf4\Delta/Pf4\Delta}$ *Mcl-1*$^{+/+}$ mice. #Morphologically recognizable megakaryocytes were enumerated in H&E-stained sternum sections from: n = 3, *Bcl-x*$^{fl/fl}$ *Mcl-1*$^{+/+}$; n = 8, *Bcl-x*$^{Pf4\Delta/Pf4\Delta}$ *Mcl-1*$^{+/+}$; n = 4, *Bcl-x*$^{Pf4\Delta/Pf4\Delta}$ *Mcl-1*$^{+/Pf4\Delta}$ mice. Data represent mean number per field of view (×200) from 10 fields per individual mouse. (B) H&E-stained BM sections. Megakaryocytes with abnormal morphology are indicated by dark blue arrows. Normal megakaryocytes are indicated by white arrows. Scale bars: 20 μm. (C) Caspase-3–positive atypical megakaryocytes present in *Bcl-x*$^{Pf4\Delta/Pf4\Delta}$ *Mcl-1*$^{+/Pf4\Delta}$ spleen. Cleaved capase-3 in brown and hematoxylin in blue. Blue arrows point to apoptotic megakaryocytes positive for active caspase-3. Note the dark pyknotic nuclei. White arrows indicate healthy megakaryocytes, negative for caspase-3. Scale bars: 20 μm. (D) Representative transmission electron microscope images of BM sections demonstrating the presence of apoptotic megakaryocytes in *Bcl-x*$^{Pf4\Delta/Pf4\Delta}$ *Mcl-1*$^{+/Pf4\Delta}$ mice. Right panels show high-magnification ultrastructure of the corresponding megakaryocytes shown in the left panels. Scale bars: 2 (white) or 10 (black) μm.

tissues, including the brain, in all *Bcl-x*$^{Pf4\Delta/Pf4\Delta}$ *Mcl-1*$^{Pf4\Delta/Pf4\Delta}$ embryos (Figure 5A-Bv-vi). Thus, *Bcl-x*$^{Pf4\Delta/Pf4\Delta}$ *Mcl-1*$^{Pf4\Delta/Pf4\Delta}$ embryos possess aberrant connections between the blood and lymphatic vascular networks, resulting in blood-filled lymphatic vessels, and in addition, exhibit focal hemorrhages, consistent with a failure of hemostasis.

Bcl-x$^{Pf4\Delta/Pf4\Delta}$ *Mcl-1*$^{Pf4\Delta/Pf4\Delta}$ fetal liver megakaryocytes are reduced in number and size

In mice, the fetal liver is the primary hematopoietic organ during embryogenesis. Megakaryocytes first appear in the liver at E11 and increase in number from E12.[30,31] To examine megakaryopoiesis in the *Bcl-x*$^{Pf4\Delta/Pf4\Delta}$ *Mcl-1*$^{Pf4\Delta/Pf4\Delta}$ fetal liver, E12.5 whole embryos were sectioned and stained with H&E. Visual inspection revealed the presence of megakaryocytes in both wild-type and mutant livers (Figure 6A). Additional staining for the specific α granule marker VWF confirmed that these cells were megakaryocytes (Figure 6B). Relative to wild-type and *Bcl-x*$^{Pf4\Delta/Pf4\Delta}$ *Mcl-1*$^{+/+}$ littermates, double knockout megakaryocytes were significantly fewer in number and appeared smaller. To quantitatively assess megakaryocyte size and number, Metamorph image processing software was used. This analysis confirmed the observation that megakaryopoiesis in the *Bcl-x*$^{Pf4\Delta/Pf4\Delta}$ *Mcl-1*$^{Pf4\Delta/Pf4\Delta}$ fetal liver is impaired (Figure 6C).

Discussion

Prior studies have demonstrated that shedding megakaryocytes and their platelet progeny absolutely require Bcl-x_L, an antiapoptotic member of the Bcl-2 protein family, to survive.[9] Bcl-x_L functions to restrain Bak and Bax, the prodeath initiators of mitochondrial damage and apoptosis. Deletion of Bcl-x_L in megakaryocytes leads to Bak/Bax-dependent apoptotic death during platelet shedding.[9] Up to the point at which proplatelet formation begins, however, Bcl-x_L–deficient megakaryocytes develop and mature normally, both in vivo and in vitro. Our work demonstrates that Mcl-1, in combination with Bcl-x_L, plays a central role in the survival of megakaryocytes.

Genetic deletion of Mcl-1 alone had no impact on the development of platelets or megakaryocytes. ABT-737 preferentially targets older platelets, and it has been suggested that this may reflect higher levels of Bcl-x_L in their younger counterparts.[7] It is conceivable that other prosurvivals, such as Mcl-1, may also be operative in young platelets. In *Mcl-1*$^{Pf4\Delta/Pf4\Delta}$ mice, platelet lifespan was normal. This is perhaps not surprising given that we could not detect Mcl-1 protein in mouse platelets, consistent with previous reports in humans.[7,15] It may be that Mcl-1, which has a short half-life in other cell types,[32] is only present in young platelets, where it might augment Bcl-x_L–mediated survival. The increased severity of thrombocytopenia in ABT-737–treated *Mcl-1*$^{Pf4\Delta/Pf4\Delta}$ mice relative to *Mcl-1*$^{+/+}$ littermates offers some support to this notion, but the observation is perhaps more likely a result of acute megakaryocyte death and concomitant failure of platelet production. Given the profound reduction in platelet lifespan caused by loss of Bcl-x_L, it will be difficult to definitively establish by genetic means whether Mcl-1 plays a role in platelet survival.

The ABT-737–induced death of Mcl-1–deficient megakaryocytes vividly illustrates the absolute dependence of megakaryocytes on Bcl-2 family prosurvival proteins. It also provides the first clear view of the morphological and ultrastructural features of acute apopototic death mediated by the classic intrinsic pathway in vivo. Previous studies have reported megakaryocyte cell death in conditions such as immune thrombocytopenia (ITP),[33] myelodysplastic syndrome (MDS),[34] and HIV infection.[35] Based on morphology, terms

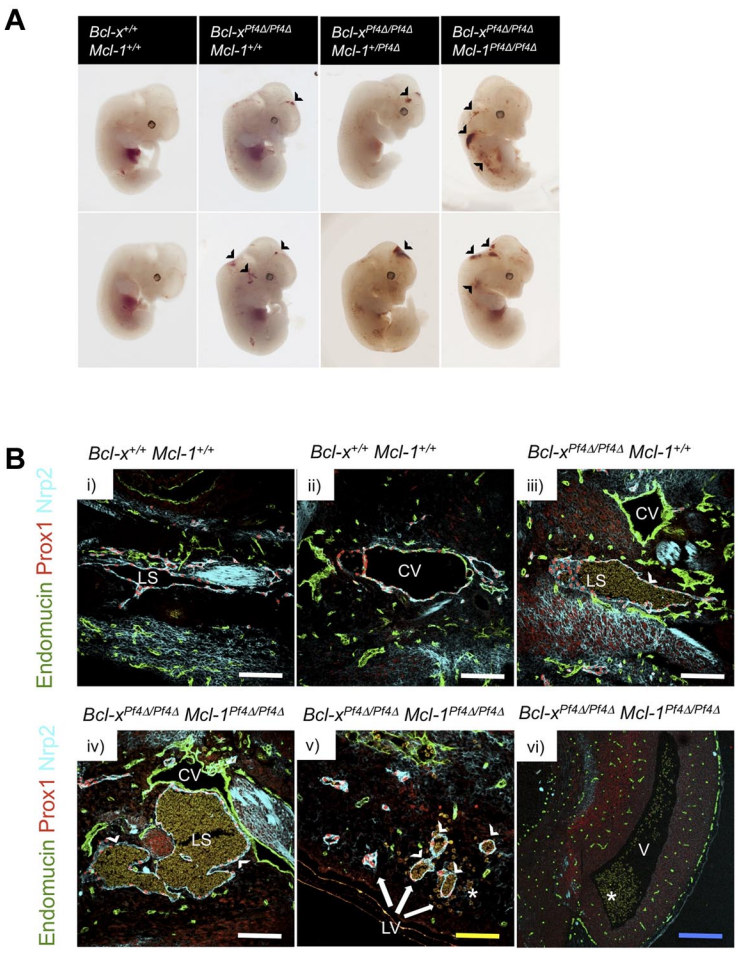

Figure 5. *Bcl-x*$^{Pf4\Delta/Pf4\Delta}$ *Mcl-1*$^{Pf4\Delta/Pf4\Delta}$ embryos exhibit hemorrhages and blood-filled lymphatic vessels. (A) Representative images from E12.5 wild-type, *Bcl-x*$^{Pf4\Delta/Pf4\Delta}$ *Mcl-1*$^{+/+}$, *Bcl-x*$^{Pf4\Delta/Pf4\Delta}$ *Mcl-1*$^{+/Pf4\Delta}$, and *Bcl-x*$^{Pf4\Delta/Pf4\Delta}$ *Mcl-1*$^{Pf4\Delta/Pf4\Delta}$ embryos. Black arrowhead indicates areas of ectopic bleeding. Note, some embryos have been tailed for genotyping. (B) Immunofluorescent detection of blood vessels and lymphatic vessels using Abs directed against endomucin (green), Prox1 (red), and neuropilin2 (Nrp2; cyan). Blood-filled lymph sacs (iii-iv) and lymphatic vessels (v) are a feature of E12.5 *Bcl-x*$^{Pf4\Delta/Pf4\Delta}$ *Mcl-1*$^{+/+}$ and *Bcl-x*$^{Pf4\Delta/Pf4\Delta}$ *Mcl-1*$^{Pf4\Delta/Pf4\Delta}$, but not wild-type (i-ii) embryos. (vi)Hemorrhages were also observed in *Bcl-x*$^{Pf4\Delta/Pf4\Delta}$ *Mcl-1*$^{Pf4\Delta/Pf4\Delta}$ embryos. Z-stack images were obtained using a Bio-Rad Radiance 2100 confocal microscope equipped with 3 lasers (488-nm Argon-ion laser, HeNe 543-nm green laser, 637-nm red diode laser) attached to an Olympus IX70 inverted microscope with UPlanApo 10×/0.40 ∞/0.17 and UApo/340 20×/0.70W ∞/0.17 objectives. Image acquisition was performed at room temperature using LaserSharp 2000 software (Version 5.2; Bio-Rad Laboratories). Adobe Photoshop CS5 (Version 12.0; Adobe) was used for subsequent image processing. LS indicates lymph sac; CV, cardinal vein; LV, lymphatic vessels; and V, ventricle. White arrowheads indicate blood-filled lymph sacs/lymphatic vessels and white asterisks (*) indicate areas of hemorrhage. Scale bars: 120 μm (white), 80 μm (yellow), and 240 μm (blue).

including necrosis, apoptosis, and para-apoptosis have been used to describe the various processes observed.[36] In comparing our observations with those published, it is interesting to note that megakaryocytes in ITP patients[33] share features similar to those of dying *Mcl-1*$^{Pf4\Delta/Pf4\Delta}$ cells. Thus, in addition to the established role of Bak/Bax-mediated apoptosis in mediating chemotherapy-induced thrombocytopenia,[9] it is possible activation of the intrinsic pathway plays a role in other disorders associated with impaired platelet production.

Megakaryocyte-specific deletion of Bcl-x_L in mice reduces their viability to ~ 80% that of wild-type littermates.[9] In this study, the additional loss of one allele of *Mcl-1* reduced the rate of survival to weaning age to only ~ 30%. Although megakaryocytes were abundant in adult *Bcl-x*$^{Pf4\Delta/Pf4\Delta}$ *Mcl-1*$^{+/Pf4\Delta}$ survivors, the presence of dying megakaryocytes exhibiting morphology similar to those in *Mcl-1*$^{Pf4\Delta/Pf4\Delta}$ mice treated with ABT-737 demonstrates that reductions in Bcl-x_L and Mcl-1 levels predispose megakaryocytes to spontaneous apoptosis in vivo. Full deletion of both Bcl-x_L and Mcl-1 disrupts megakaryopoiesis. Fetal livers in E12.5 *Bcl-x*$^{Pf4\Delta/Pf4\Delta}$ *Mcl-1*$^{Pf4\Delta/Pf4\Delta}$ double knockout embryos show a significant reduction in the number and size of megakaryocytes, suggesting that larger, mature cells cannot develop. Decreases in prosurvival signaling during megakaryocyte development presumably increase the risk of stochastic cell death, particularly as the stresses engendered by polyploidization and cytoplasmic maturation intensify. At least in the fetus, however, loss of Mcl-1 and Bcl-x_L does not completely abrogate megakaryocyte development. Because *Bcl-x*$^{Pf4\Delta/Pf4\Delta}$ *Mcl-1*$^{Pf4\Delta/Pf4\Delta}$ mice do not survive to adulthood, it remains to be determined whether this reflects the differential requirements of fetal and adult megakaryopoiesis,[37] or a potential role for other Bcl-2 family proteins in the survival of developing megakaryocytes. Given that ABT-737 also targets Bcl-2, the latter possibility will be worth investigating.

The BH3 mimetic drug navitoclax (ABT-263) is an orally available derivative of ABT-737, with overlapping target specificity and potency, currently in clinical trials for lymphoid malignancies.[11,17,18] It causes thrombocytopenia in patients, and lead-in dosing schedules have been developed to circumvent the severity of this on-target toxicity. While demonstrating promising antitumor activity as a single agent, navitoclax is likely to be used in combination with standard chemotherapeutic agents. Preclinical studies indicate that navitoclax synergizes with agents such as erlotinib and docetaxel, and that this is associated with neutralization of Mcl-1.[38] Our results suggest that therapeutic approaches targeting both Bcl-x_L and Mcl-1 would have severe effects on the megakaryocyte lineage because both platelets and megakaryocytes would be impacted. This might also be true of megakaryocyte progenitors, although the role of prosurvival proteins in these cells is unclear, because the timing of deletion mediated by *platelet factor 4* Cre has not been specifically pinpointed. Clearly, further investigations are required to fully delineate the role of the Bcl-2 family in regulating the survival of the megakaryocyte lineage, both at steady state and in response to insult. This is particularly pertinent given ongoing efforts to specifically target prosurvival proteins in a range of human malignancies.[39-41]

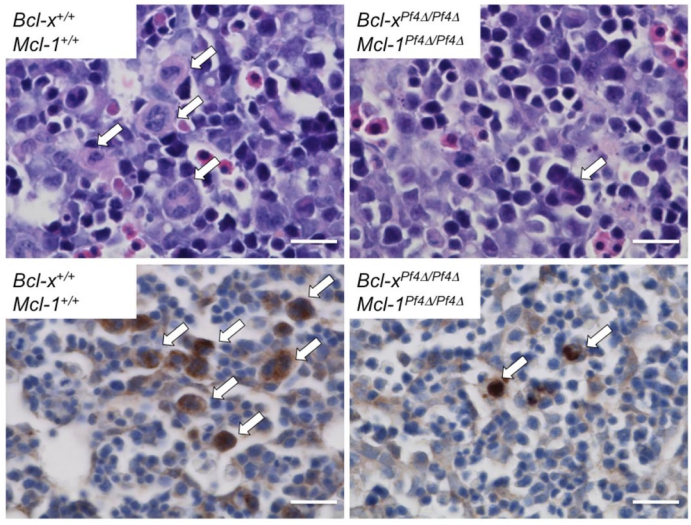

C

	Bcl-x+/+ Mcl-1+/+ n=4	Bcl-x Pf4Δ/Pf4Δ Mcl-1+/+ n=5	Bcl-x Pf4Δ/Pf4Δ Mcl-1Pf4Δ/Pf4Δ n=4
Number	13 ± 6	12 ± 3	8 ± 2*
Width	16.2 ± 1.8	14.6 ± 1.4	13.3 ± 0.2*
Height	16.3 ± 0.9	14.9 ± 1.9	13.9 ± 0.8**
Area	192 ± 21	164 ± 39	141 ± 6**
Perimeter	53.4 ± 3.6	49.1 ± 5.0	45.0 ± 1.0**

Figure 6. *Bcl-x*$^{Pf4\Delta/Pf4\Delta}$ *Mcl-1*$^{Pf4\Delta/Pf4\Delta}$ fetal liver megakaryocytes are reduced in number and size. (A) Representative images of H&E-stained E12.5 fetal liver sections. White arrows indicate megakaryocytes. Scale bar: 20 μm. Images were acquired on a Nikon Eclipse E600 microscope equipped with AxioCam MRc5 (Zeiss) and AxioVision 4.8. Scale bars were inserted with ImageJ 1.42q. (B) Representative images of E12.5 fetal liver sections stained with anti-VWF (brown). White arrows indicate megakaryocytes. Images were acquired as in panel A. Scale bar: 20 μm. (C) Megakaryocytes were enumerated and width (μm), height (μm), area (μm^2), and perimeter (μm) determined from 5-7 separate images of H&E-stained E12.5 fetal liver sections/embryo using Metamorph image processing software (Version 7.0). n = 4, *Bcl-x*$^{+/+}$*Mcl-1*$^{+/+}$; n = 5, *Bcl-x*$^{Pf4\Delta/Pf4\Delta}$ *Mcl-1*$^{+/+}$; and n = 4, *Bcl-x*$^{Pf4\Delta/Pf4\Delta}$ *Mcl-1*$^{Pf4\Delta/Pf4\Delta}$ embryos. Data represent mean ± SD.

Acknowledgments

The authors thank Jason Corbin, Ladina Di Rago, Sandra Mifsud, and Maria Kauppi for excellent technical assistance; WEHI Bioservices for outstanding animal husbandry; Czesia Markiewicz for photography; Philippe Bouillet, Douglas Green, Lothar Hennighausen, Radek Skoda, and Andreas Strasser for providing mouse strains; Abbott Laboratories for ABT-737; and David Huang for insightful discussions.

This work was supported by a Project grant (575535), a Program grant (461219), and an Independent Research Institutes Infrastructure Support Scheme grant (361646) from the Australian National Health and Medical Research Council (NHMRC); Fellowships from the Sylvia and Charles Viertel Foundation (B.T.K.), the Leukemia & Lymphoma Society (E.C.J.), NHMRC/Inserm (C.J.), EMBO (C.J.), NHMRC (A.W.R., B.T.K.); the Cancer Council of Victoria (D.M.) and the National Heart Foundation (N.L.H.); the Australian Cancer Research Fund, and a Victorian State Government Operational Infrastructure Support grant.

Authorship

Contribution: M.A.D., E.C.J., C.J., and B.T.K. designed research, analyzed data, and wrote the manuscript; M.A.D., E.C.J., C.J., K.J.H., S.E., M.L., K.L.B., R.M.L., K.L.R., N.L.H., and D.M. performed research and analyzed data; and M.J.W. and A.W.R. designed research.

Conflict-of-interest disclosure: The WEHI has an ongoing research collaboration agreement with Genentech in the field of Bcl-2 proteins. The work described in this manuscript was not funded by either Genentech or Abbott Laboratories. The authors declare no competing financial interests.

The current affiliation for C.J. is Center de Référence des Pathologies Plaquettaires, Laboratoire d'hématologie, CHU de Bordeaux (Bordeaux, France); Université Bordeaux Segalen (Bordeaux, France); Inserm U1034 (Pessac, France).

Correspondence: Benjamin T. Kile, Cancer and Hematology Division, The Walter and Eliza Hall Institute of Medical Research, 1G Royal Parade, Parkville 3052, Victoria, Australia; e-mail: kile@wehi.edu.au.

References

1. Junt T, Schulze H, Chen Z, et al. Dynamic visualization of thrombopoiesis within bone marrow. *Science.* 2007;317(5845):1767-1770.
2. Italiano J, Lecine P, Shivdasani R, Hartwig J. Blood platelets are assembled principally at the ends of proplatelet processes produced by differentiated megakaryocytes. *J Cell Biol.* 1999; 147(6):1299-1312.
3. Becker RP, De Bruyn PP. The transmural passage of blood cells into myeloid sinusoids and the entry of platelets into the sinusoidal circulation; a scanning electron microscopic investigation. *Am J Anat.* 1976;145(2):183-205.
4. Leeksma C, Cohen J. Determination of the life of human blood platelets using labelled diisopropylfluorophosphanate. *Nature.* 1955;175(4456):552-553.
5. Ault KA, Knowles C. In vivo biotinylation demonstrates that reticulated platelets are the youngest platelets in circulation. *Exp Hematol.* 1995;23(9): 996-1001.
6. Youle RJ, Strasser A. The BCL-2 protein family: opposing activities that mediate cell death. *Nat Rev Mol Cell Biol.* 2008;9(1):47-59.
7. Mason KD, Carpinelli MR, Fletcher JI, et al. Programmed anuclear cell death delimits platelet life span. *Cell.* 2007;128(6):1173-1186.
8. Kodama T, Takehara T, Hikita H, et al. Thrombocytopenia exacerbates cholestasis-induced liver fibrosis in mice. *Gastroenterology.* 2010;138(7): 2487-2498.
9. Josefsson EC, James C, Henley KJ, et al. Megakaryocytes possess a functional intrinsic apoptosis pathway that must be restrained to survive and produce platelets. *J Exp Med.* 2011;208(10): 2017-2031.
10. Oltersdorf T, Elmore SW, Shoemaker AR, et al.

An inhibitor of Bcl-2 family proteins induces regression of solid tumours. *Nature.* 2005;435(7042):677-681.

11. Tse C, Shoemaker AR, Adickes J, et al. ABT-263: a potent and orally bioavailable Bcl-2 family inhibitor. *Cancer Res.* 2008;68(9):3421-3428.
12. Dasgupta SK, Argaiz ER, Mercado JE, et al. Platelet senescence and phosphatidylserine exposure. *Transfusion.* 2010;50(10):2167-2175.
13. Schoenwaelder SM, Yuan Y, Josefsson EC, et al. Two distinct pathways regulate platelet phosphatidylserine exposure and procoagulant function. *Blood.* 2009;114(3):663-666.
14. Vogler M, Hamali HA, Sun XM, et al. BCL2/BCL-XL inhibition induces apoptosis, disrupts cellular calcium homeostasis, and prevents platelet activation. *Blood.* 2011;117(26):7145-7154.
15. Zhang H, Nimmer PM, Tahir SK, et al. Bcl-2 family proteins are essential for platelet survival. *Cell Death Differ.* 2007;14(5):943-951.
16. Schoenwaelder SM, Jarman KE, Gardiner EE, et al. Bcl-xL-inhibitory BH3 mimetics can induce a transient thrombocytopathy that undermines the hemostatic function of platelets. *Blood.* 2011;118(6):1663-1674.
17. Roberts AW, Seymour JF, Brown JR, et al. Substantial susceptibility of chronic lymphocytic leukemia to BCL2 inhibition: results of a phase I study of navitoclax in patients with relapsed or refractory disease. *J Clin Oncol.* 2012;30(5):488-496.
18. Wilson WH, O'Connor OA, Czuczman MS, et al. Navitoclax, a targeted high-affinity inhibitor of BCL-2, in lymphoid malignancies: a phase 1 dose-escalation study of safety, pharmacokinetics, pharmacodynamics, and antitumour activity. *Lancet Oncol.* 2010;11(12):1149-1159.
19. Dzhagalov I, St John A, He Y. The antiapoptotic protein Mcl-1 is essential for the survival of neutrophils but not macrophages. *Blood.* 2007;109(4):1620-1626.
20. Opferman J, Iwasaki H, Ong C, et al. Obligate role of anti-apoptotic MCL-1 in the survival of hematopoietic stem cells. *Science.* 2005;307(5712):1101-1104.
21. Opferman J, Letai A, Beard C, Sorcinelli M, Ong C, Korsmeyer S. Development and maintenance of B and T lymphocytes requires antiapoptotic MCL-1. *Nature.* 2003;426(6967):671-676.
22. Rucker EB, 3rd Dierisseau P, Wagner KU, et al. Bcl-x and Bax regulate mouse primordial germ cell survival and apoptosis during embryogenesis. *Mol Endocrinol.* 2000;14(7):1038-1052.
23. Tiedt R, Schomber T, Hao-Shen H, Skoda RC. Pf4-Cre transgenic mice allow the generation of lineage-restricted gene knockouts for studying megakaryocyte and platelet function in vivo. *Blood.* 2007;109(4):1503-1506.
24. Alexander W, Roberts A, Nicola N, Li R, Metcalf D. Deficiencies in progenitor cells of multiple hematopoietic lineages and defective megakaryocytopoiesis in mice lacking the thrombopoietic receptor c-Mpl. *Blood.* 1996;87(6):2162-2170.
25. Kruse EA, Loughran SJ, Baldwin TM, et al. Dual requirement for the ETS transcription factors Fli-1 and Erg in hematopoietic stem cells and the megakaryocyte lineage. *Proc Natl Acad Sci U S A.* 2009;106(33):13814-13819.
26. Aster RH, Jandl JH. Platelet sequestration in man. I. Methods. *J Clin Invest.* 1964;43:843-855.
27. Dowling MR, Josefsson EC, Henley KJ, Hodgkin PD, Kile BT. Platelet senescence is regulated by an internal timer, not damage inflicted by hits. *Blood.* 2010;116(10):1776-1778.
28. Bertozzi CC, Schmaier AA, Mericko P, et al. Platelets regulate lymphatic vascular development through CLEC-2-SLP-76 signaling. *Blood.* 2010;116(4):661-670.
29. Carramolino L, Fuentes J, Garcia-Andres C, Azcoitia V, Riethmacher D, Torres M. Platelets play an essential role in separating the blood and lymphatic vasculatures during embryonic angiogenesis. *Circ Res.* 2010;106(7):1197-1201.
30. Matsumura G, Sasaki K. The ultrastructure of megakaryopoietic cells of the yolk sac and liver in mouse embryo. *Anat Rec.* 1988;222(2):164-169.
31. Tober J, Koniski A, McGrath KE, et al. The megakaryocyte lineage originates from hemangioblast precursors and is an integral component both of primitive and of definitive hematopoiesis. *Blood.* 2007;109(4):1433-1441.
32. Nijhawan D, Fang M, Traer E, et al. Elimination of Mcl-1 is required for the initiation of apoptosis following ultraviolet irradiation. *Genes Dev.* 2003;17(12):1475-1486.
33. Houwerzijl E, Blom N, van der Want J, et al. Ultrastructural study shows morphologic features of apoptosis and para-apoptosis in megakaryocytes from patients with idiopathic thrombocytopenic purpura. *Blood.* 2004;103(2):500-506.
34. Houwerzijl EJ, Blom NR, van der Want JJL, et al. Increased peripheral platelet destruction and caspase-3-independent programmed cell death of bone marrow megakaryocytes in myelodysplastic patients. *Blood.* 2005;105(9):3472-3479.
35. Zauli G, Catani L, Gibellini D, et al. Impaired survival of bone marrow GPIIb/IIa+ megakaryocytic cells as an additional pathogenetic mechanism of HIV-1-related thrombocytopenia. *Br J Haematol.* 1996;92(3):711-717.
36. Houwerzijl EJ, Blom NR, van der Want JJL, Vellenga E, de Wolf JTM. Megakaryocytic dysfunction in myelodysplastic syndromes and idiopathic thrombocytopenic purpura is in part due to different forms of cell death. *Leukemia.* 2006;20(11):1937-1942.
37. Liu ZJ, Italiano J Jr, Ferrer-Marin F, et al. Developmental differences in megakaryocytopoiesis are associated with up-regulated TPO signaling through mTOR and elevated GATA-1 levels in neonatal megakaryocytes. *Blood.* 2011;117(15):4106-4117.
38. Chen J, Jin S, Abraham V, et al. The Bcl-2/Bcl-X(L)/Bcl-w inhibitor, navitoclax, enhances the activity of chemotherapeutic agents in vitro and in vivo. *Mol Cancer Ther.* 2011;10(12):2340-2349.
39. Leber B, Geng F, Kale J, Andrews DW. Drugs targeting Bcl-2 family members as an emerging strategy in cancer. *Expert Rev Mol Med.* 2010;12:e28.
40. Lessene G, Czabotar PE, Colman PM. BCL-2 family antagonists for cancer therapy. *Nat Rev Drug Discov.* 2008;7(12):989-1000.
41. Petros AM, Huth JR, Oost T, et al. Discovery of a potent and selective Bcl-2 inhibitor using SAR by NMR. *Bioorg Med Chem Lett.* 2010;20(22):6587-6591.